This article was downloaded by: [Institute Of Atmospheric Physics]
On: 09 December 2014, At: 15:27
Publisher: Taylor & Francis
Informa Ltd Registered in England and Wales Registered Number: 1072954 Registered office: Mortimer House, 37-41 Mortimer Street, London W1T 3JH, UK

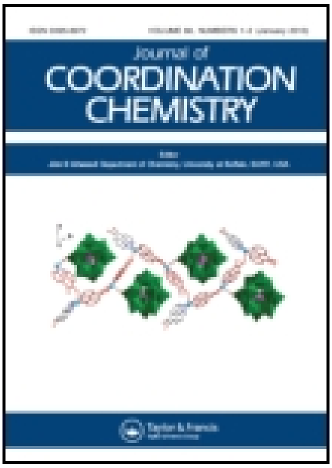

Click for updates

Journal of Coordination Chemistry
Publication details, including instructions for authors and subscription information:
http://www.tandfonline.com/loi/gcoo20

Synthesis, characterization, and reactivity of self-assembled tetranuclear arene ruthenium metalla-rectangles

Ai-Quan Jia[a], Min Chen[a], Li-Miao Shi[a], Hua-Tian Shi[a] & Qian-Feng Zhang[a]

[a] Institute of Molecular Engineering and Applied Chemistry, Anhui University of Technology, Ma'anshan, PR China

Accepted author version posted online: 18 Sep 2014.Published online: 08 Oct 2014.

To cite this article: Ai-Quan Jia, Min Chen, Li-Miao Shi, Hua-Tian Shi & Qian-Feng Zhang (2014) Synthesis, characterization, and reactivity of self-assembled tetranuclear arene ruthenium metalla-rectangles, Journal of Coordination Chemistry, 67:22, 3565-3577, DOI: 10.1080/00958972.2014.966703

To link to this article: http://dx.doi.org/10.1080/00958972.2014.966703

PLEASE SCROLL DOWN FOR ARTICLE

Taylor & Francis makes every effort to ensure the accuracy of all the information (the "Content") contained in the publications on our platform. However, Taylor & Francis, our agents, and our licensors make no representations or warranties whatsoever as to the accuracy, completeness, or suitability for any purpose of the Content. Any opinions and views expressed in this publication are the opinions and views of the authors, and are not the views of or endorsed by Taylor & Francis. The accuracy of the Content should not be relied upon and should be independently verified with primary sources of information. Taylor and Francis shall not be liable for any losses, actions, claims, proceedings, demands, costs, expenses, damages, and other liabilities whatsoever or howsoever caused arising directly or indirectly in connection with, in relation to or arising out of the use of the Content.

This article may be used for research, teaching, and private study purposes. Any substantial or systematic reproduction, redistribution, reselling, loan, sub-licensing, systematic supply, or distribution in any form to anyone is expressly forbidden. Terms &

Journal of Coordination Chemistry, 2014
Vol. 67, No. 22, 3565–3577, http://dx.doi.org/10.1080/00958972.2014.966703

Synthesis, characterization, and reactivity of self-assembled tetranuclear arene ruthenium metalla-rectangles

AI-QUAN JIA*, MIN CHEN, LI-MIAO SHI, HUA-TIAN SHI
and QIAN-FENG ZHANG*

Institute of Molecular Engineering and Applied Chemistry, Anhui University of Technology,
Ma'anshan, PR China

(*Received 30 May 2014; accepted 28 August 2014*)

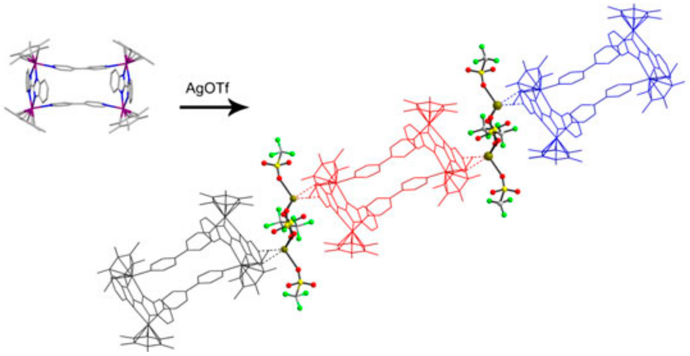

A 1-D coordination network $\{[Ru_4(\eta^6\text{-}C_6Me_6)_4(bpy)_2(BiBzIm)_2{\cdot}Ag_2(OTf)_4]^{2+}\}_n$ containing silver triflate interaction was synthesized *via* self-assembly of $[(C_6Me_6)RuCl_2]_2$, 4,4′-bipyridine, and 2,2′-bisbenzimidazole in the presence of excess AgOTf or through direct reaction of metalla-rectangle $[Ru_4(C_6Me_6)_4(bpy)_2(BiBzIm)_2]^{4+}$ and AgOTf.

Self-assembly of 4,4′-bipyridine (bpy) with arene-ruthenium building blocks and 2,2′-bisbenzimidazole ($H_2BiBzIm$) in the presence of AgOTf ($OTf = OSO_2CF_3$) afforded tetranuclear cations of the type $[Ru_4(\eta^6\text{-arene})_4(bpy)_2(BiBzIm)_2]^{4+}$ (arene = $p\text{-}^iPrC_6H_4Me$ **1**, C_6Me_6 **2**), while similar reactions by use of $[(\eta^6\text{-}C_6Me_6)Ru(\mu\text{-Cl})Cl]_2$ and excess AgOTf led to isolation of a cationic coordination network $\{[Ru_4(\eta^6\text{-}C_6Me_6)_4(bpy)_2(BiBzIm)_2{\cdot}Ag_2(OTf)_4]^{2+}\}_n$ (**3**), which could also be obtained by treatment of [**2**][OTf]$_4$ with AgOTf in methanol. Complex **3** is constructed by π coordination of BiBzIm(η^2-carcon) with Ag(I). The coordination geometry around the silver(I) ion is pseudo-tetrahedral (taking the C=C group as one ligand). Self-assembly of only two components: $[(\eta^6\text{-}C_6Me_6)Ru(\mu\text{-Cl})Cl]_2$ reacted with the 3-pyridyl-bian (*m*Py-bian) linker in the presence of limited AgOTf to give a chloro-bridged metalla-rectangle $[Ru_4(\eta^6\text{-}C_6Me_6)_4(\mu\text{-Cl})_4(m\text{Py-bian})_2Ag]^{5+}$ (**4**), which enclosed a silver in the center. The coordination geometry around silver(I) in **4** is unusual square planar. The molecular structures of **1–4** were confirmed by X-ray crystallography along with other spectroscopic properties.

Keywords: Ruthenium; Silver; Heterometallic; Metallamacrocycles; X-ray structure

---

*Corresponding authors. Email: jaiquan@ahut.edu.c (A.-Q. Jia); zhangqf@ahut.edu.cn (Q.-F. Zhang)

1. Introduction

Metallo-supramolecular complexes have attracted attention for intriguing structures [1], potential electronic [2], magnetic [3], host-guest [4], drug delivery [5], and catalytic properties [6]. These have driven development to systematic and rational approaches for their construction with desirable shapes, sizes, and ultimately functions [7]. One successful strategy for designing metal-containing supramolecules is to employ quasi-octahedral geometries that bear arene or cyclopentadienyl groups as building blocks. These (arene)-Ru or (cyclopentadienyl)-Ir/Rh complexes have good solubility in common solvents and have three available coordination sites which could be tuned to construct metallamacrocyclic complexes as well as coordination cages [8, 9]. Various polynuclear arene ruthenium systems, such as tetranuclear rectangular molecules, hexanuclear prisms, and octanuclear organometallic boxes, have been reported by several groups [10–15]. Attention has been focused on synthesis of homometallic macrocycles, whereas the chemistry, as well as the synthetic strategy toward heterometallic frameworks, has received much less attention [16, 17]. Synthesis of multimetallic hybrid materials is of special interest because the incorporation of two or more kinds of metal ions can add different functionalities [16, 17]. For example, Cp*Rh-based heterometallic metalla-rectangle $\{(Cp^*Rh)_4(bpe)_2[Cu(opba)]_2\}^{4+}$ (Cp* = cyclopentadienyl, bpe = 1,2-bis(4-pyridyl)ethylene, opba = *o*-phenylenebis-(oxamato) shows extraordinary catalytic abilities with high efficiency and wide substrate selectivity in the acyl-transfer reaction arising from the combination of open copper centers and favorable cavity space [7].

Ag(I) has been extensively used for formation of coordination networks due to its weak stereochemical demands [18, 19]. There is growing literature reporting the formation of stable crystalline Ag–arene π-complexes with the arene bonded in a η^1-, η^2-, η^3- and/or η^6-coordination mode, of which the η^2-mode is more common [20–22]. The aromatic rings include benzene, cyclophane, indene, acenaphthene, naphthalene, anthracene, as well as pyrene and perylene [23]. However, π coordination of Ag(I) with *N*-containing heterocycles has rarely been reported. A related complex is $\{[AgL][OTf]_2\}_n$ (L = 2,2-bis-pyridin-2-ylmethyl-2,3-dihydro-1H-isoindolium), which bears a cationic ligand [24]. The silver(I) ions might come from various silver(I) salts, such as $AgClO_4$, AgOTf, and AgO_2CCF_3. Usually, silver(I) triflate is more popular due to its easy manipulation and rich coordination modes as shown in Chart 1; as a result, many neutral or cationic structurally diverse Ag–arene π-complexes containing silver triflate were synthesized and investigated [25–27]. Herein we describe the synthesis and characterization of two homonuclear arene-ruthenium metalla-rectangles, a 1-D heterometallic coordination network constructed by Ag–arene(*N*-heterocycle) π bonds, and a chloro-bridged Ru/Ag metalla-rectangle containing a Ag-diimine moiety (scheme 1).

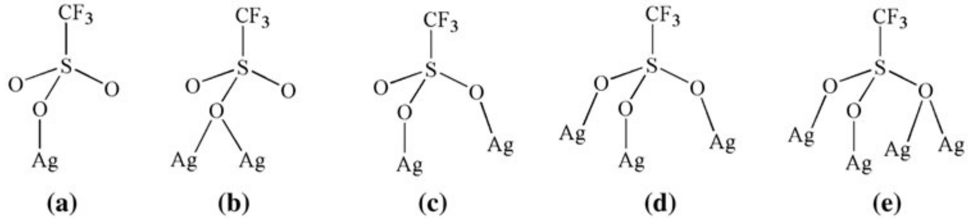

Chart 1. Coordination modes of $^{-}$OTF to silver(I).

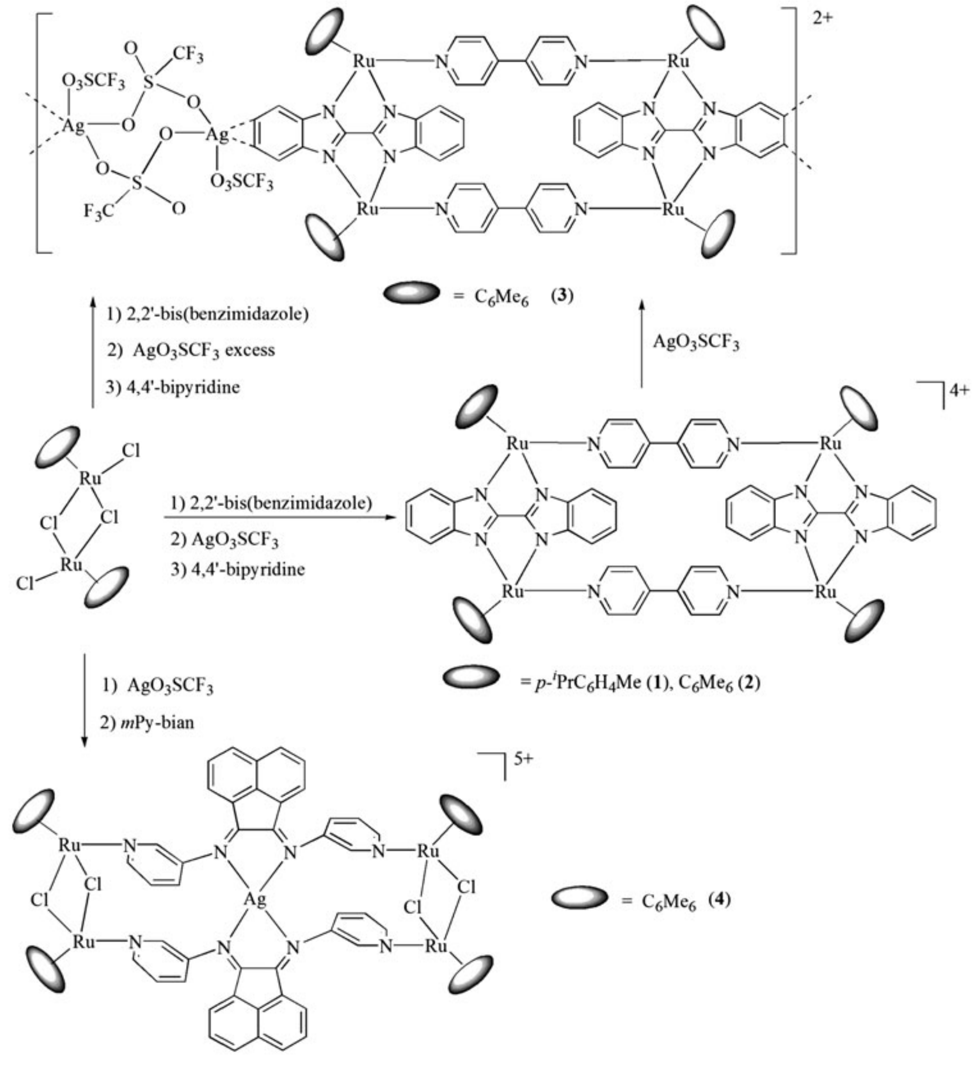

Scheme 1. Syntheses of **1–4**.

2. Results and discussion

Assembly of $[(p\text{-}^i\text{PrC}_6\text{H}_4\text{Me})\text{RuCl}_2]_2$ or $[(\text{C}_6\text{Me}_6)\text{RuCl}_2]_2$ with 2,2′-bisbenzimidazole (H_2BiBzIm) and 4,4′-bipyridine (bpy) in the presence of four equiv. of AgOTf afforded tetranuclear metalla-rectangles $[\text{Ru}_4(\text{arene})_4(\text{bpy})_2(\text{BiBzIm})_2]^{4+}$ (arene = $p\text{-}^i\text{PrC}_6\text{H}_4\text{Me}$ **1**, C_6Me_6 **2**) as orange crystals in good yields. Compared with the already known frameworks $[(\text{Ir/Rh})_4\text{Cp*}_4(\text{bpy})_2(\text{BiBzIm})_2]^{4+}$ [28], a different synthetic method was employed to obtain **1** and **2**. First, the arene ruthenium building block and H_2BiBzIm were mixed in methanol and stirred for 6 h, then four equiv. of AgOTf was added to remove the chlorides, and then bpy was added to form the tetranuclear metalla-rectangle **1** or **2**. In the previous report, $[Cp^*Ir/RhCl_2]_2$ and bpy were mixed first to form the known dinuclear complex $[\{Cp^*Ir/RhCl_2\}_2(bpy)]$, then AgOTf and $H_2BiBzIm$ were sequentially added to form metalla-rectangles $[(Ir/Rh)_4Cp^*_4(bpy)_2(BiBzIm)_2]^{4+}$. The new synthetic route is more efficient to obtain the metalla-rectangles in good yield (*ca.* 80%) compared with the literature method (*ca.* 65%) [28].

Similar reaction using $[(C_6Me_6)RuCl_2]_2$ and excess AgOTf in methanol led to isolation of a 1-D, mixed-metal network $\{[Ru_4(C_6Me_6)_4(bpy)_2(BiBzIm)_2\cdot Ag_2(OTf)_4]^{2+}\}_n$ (**3**), which could aslo be obtained by direct reaction of **2** with two equiv. of AgOTf in methanol. In **3**, the discrete metalla-rectangles are linked by $[Ag_2(OTf)_4]]^{2-}$ cores via Ag–arene π bonds to form a 1-D chain. The two silver ions in $[Ag_2(OTf)_4]^{2-}$ are connected by two bridging $^{-}$OTf anions in a μ_2,η^2-coordination mode (type **c**). Attempts to synthesize the $\{[Ru_4(p\text{-}^iPrC_6H_4Me)_4(bpy)_2(BiBzIm)_2\cdot Ag_2(OTf)_4]^{2+}\}_n$ failed, possibly due to less electron density on the BiBzIm ring. An infinite tubular network $\{[Cp^*Ir(L)]_4\cdot AgNO_3\cdot H_2O\}_n$ (HL = 2,4-diacetyl-5-hydroxy-5-methyl-3-(3-pyridinyl)-cyclohexanone) was reported by Jin, based on the interconnection of metallamacrocycles $[Ir_4]$ by silver coordination to a functional "third site" (i.e. $O_{carbonyl}$–Ag–$O_{carbonyl}$), and the silver(I) ion is coordinated by four oxygens from two carbonyl groups, one water, and one nitrate [19]. The organometallic Ag–arene(BiBzIm) π bonds, instead of Ag–$O_{carbonyl}$ coordination bonds, connected the metalla-rectangles in **3**, which is quite rare for metal-containing supramolecules.

Previously, Jin reported that treatment of $[\{Cp^*IrCl_2\}_2(bpy)]$ with two equiv. of AgOTf or $AgBF_4$ afforded chloro-bridged tetranuclear complex $[\{Cp^*_2Ir_2(\mu\text{-}Cl)_2\}_2(bpy)_2]^{4+}$ [29]. Moreover, Therrien reported that the dinuclear (arene)ruthenium complexes $[Ru(arene)Cl_2]_2$ reacted with 2,4,6-tris(pyridinyl)-1,3,5-triazine (tpt) in the presence of two equiv. of AgOTf to form chloro-bridged hexanuclear cations $[Ru_6(arene)_6(\mu_3\text{-tpt-}\kappa N)_2(\mu\text{-}Cl)_6]^{6+}$ [11]. It prompts us to explore the self-assembly of $[(C_6Me_6)RuCl_2]_2$ and the bis(pyridyl)(α-diimine) ligand (*m*Py-bian) in the presence of three equiv. of AgOTf in methanol, which resulted in formation of a chloro-bridged heterometallic metalla-rectangle $[Ru_4(C_6Me_6)_4(\mu\text{-}Cl)_4(m\text{Py-bian})_2Ag]^{5+}$ (**4**). The silver(I) is enclosed in the metalla-rectangle by coordinating to two α-diimine groups. A similar framework is $[Cp^*_4Ir_4(BiBzIm)_2(m\text{Py-bian})_2Ag(H_2O)]^{5+}$, which was synthesized by stepwise reaction of $[Cp^*IrCl_2]_2$, $H_2BiBzIm$, and *m*Py-bian in the presence of excess AgOTf. The encapsulated silver(I) ion is five-coordinate by four nitrogens from two α-diimine groups and one water [28]. The isolation of chloro-bridged **3** indicates that Ag(I) coordination occurred prior to the formation of the supposed intermediate $[Cp^*_4Ir_4(BiBzIm)_2(m\text{Py-bian})_2]^{4+}$ [28]. Self-assembly of $[Ru(arene)Cl_2]_2$ with *m*Py-bian and other metal ions in the presence of limited silver(I) salt to form other heterometallic metalla-rectangles is underway.

The ^{1}H NMR spectrum of **1** clearly shows symmetrical geometry in solution. One group of $p\text{-}^iPrC_6H_4Me$ signals is observed, appearing at 0.90 (d, J = 6.8 Hz, $CH(CH_3)_2$), 1.65 (s, $ArCH_3$), 2.46 (sept, 4H, $CH(CH_3)_2$), 6.17 (d, J = 6.4 Hz), 6.62 (d, J = 6.0 Hz) ppm, respectively. The resonances of bpy protons are two doublets appearing at 7.06 (d, J = 6.4 Hz) and 7.81 (d, J = 6.4 Hz) ppm. The BiBzIm ring protons are two quartets at 7.59 (q, J = 3.2 Hz) and 8.10 (q, J = 3.2 Hz) ppm, shifted downfield compared with those in $[\{Re(CO)_3\}_4(bpy)_2(BiBzIm)_2]$ (7.36 and 7.73 ppm, q, J = 3 Hz) [30]. The ^{13}C NMR spectrum of **1** further confirms its symmetrical structure, three high field singlets at 18.04, 22.57, and 32.67 ppm are assigned to three different alkyl carbons in $p\text{-}Pr^iC_6H_4Me$ and four singlets at 79.80, 87.38, 103.86, and 104.48 ppm are attributed to the four different aryl carbons in $p\text{-}^iPrC_6H_4Me$. The C=N resonance of bpy and N=C–N resonance of BiBzIm are at 155.11 and 157.68 ppm, respectively, which compare well with those in $[\{Re(CO)_3\}_4(bpy)_2$

(BiBzIm)$_2$] [30] and [Ru$_4$(C$_6$Me$_6$)$_4$(bpy)$_2$(2,5-dichloro-1,4-benzoquinonato)$_2$]$^{4+}$ [10]. Similarly, only one singlet at 2.26 ppm (C$_6$*Me*$_6$) in ^{1}H NMR spectrum and two singlets at 17.09 (C$_6$*Me*$_6$) and 96.19 (*C*$_6$Me$_6$) ppm are found in ^{13}C NMR spectrum of **2**. The resonances of bpy protons in **2** at 6.97 (d, $J = 6.8$ Hz) and 7.72 (d, $J = 6.8$ Hz) ppm shift upfield 0.09 ppm compared with those in **1** (7.06 and 7.81 ppm). Moreover, the resonances of BiBzIm protons in **2** at 7.52 and 7.95 ppm also shift upfield 0.07 and 0.15 ppm, respectively, compared with those in **1** (7.59 and 8.10 ppm), suggesting that different arene ruthenium building blocks do have influence on the electron density of bpy and BiBzIm. The C=N resonance of bpy and N=C–N resonance of BiBzIm in **2** are at 154.30 and 157.85 ppm, respectively, similar to those in **1** (155.11 and 157.68 ppm). The BiBzIm proton resonances (7.63 and 7.96 ppm) in **3** shift upfield 0.11 and 0.02 ppm, respectively, compared to those in **2** (7.52 and 7.94 ppm), as a result of Ag–arene coordination [31]. The ^{1}H NMR spectrum of **4** displays C$_6$*Me*$_6$ signals as a singlet at 2.24 ppm, similar to that in **2**. The infrared spectra of **1–4** show C=N absorptions around 1620 cm^{-1}, which compare well with related complexes [10, 28]. A slightly lower frequency at 1479 cm^{-1} [ν(C=C)] compared with that of **2** (1481 cm^{-1}) was found, suggesting interactions of silver(I) to carbon-carbon π bonds of BiBzIm rings.

The structures of **1–4** were established by X-ray diffraction. The ORTEP representations with selected interatomic distances and angles are shown in figures 1–3 and figure 5, respectively. Self-assembly of bpy with p-^{i}PrC$_6$H$_4$Me ruthenium building block and H$_2$BiBzIm in the presence of four equiv. of AgOTf afforded orange crystals as [**1**][OTf]$_4$·4CH$_3$OH [figure 1(a)], while similar reaction by use of excess AgOTf gave orange crystals identified as [**1**][OTf]$_4$ [figure 1(b)] instead of the expected mixed-metal 1-D chain. In [**1**][OTf]$_4$·4-CH$_3$OH for example, each Ru is coordinated by one nitrogen from bpy and two nitrogens from BiBzIm, resulting in a somewhat distorted rectangle structure, with the dimensions 11.26 × 5.58 Å, as defined by the ruthenium centers, and the Ru···Ru diagonal lengths in the rectangular structure are 12.77 and 12.37 Å, respectively. One methanol guest molecule is found inside the cavity of **1**, one methanol is outside the cavity, and the other two methanols are omitted using the SQUEEZE algorithm due to disorder. The similar distorted rectangle structure **2** (dimensions: 11.27 × 5.60 Å, figure 2) has almost the same Ru···Ru

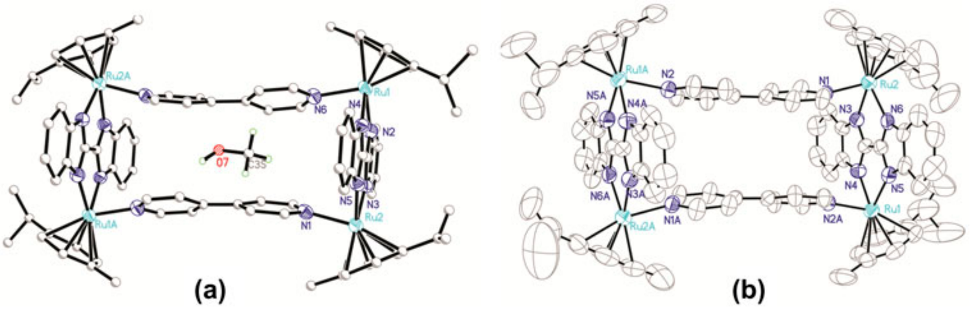

Figure 1. Molecular structures of **1**·4CH$_3$OH (a) and **1** (b) with thermal ellipsoids drawn at the 30% level. Hydrogens are omitted for clarity except methanol guest molecule in **1**·4CH$_3$OH. Selected distances (Å) and angles (°): for **1**·4CH$_3$OH, Ru(1)–N(6) 2.129(6), Ru(1)–N(2) 2.149(7), Ru(1)–N(4) 2.165(6), Ru(2)–N(1) 2.129(7), Ru(2)–N(3) 2.149(7), Ru(2)–N(5) 2.178(7); N(2)–Ru(1)–N(4) 79.2(3), N(4)–Ru(1)–N(6) 81.8(3), N(2)–Ru(1)–N(6) 85.9(3), N(3)–Ru(2)–N(5) 79.7(2). For **1**, Ru(1)–N(2A) 2.126(6), Ru(1)–N(5) 2.134(7), Ru(1)–N(4) 2.151(6), Ru(2)–N(1) 2.141(6), Ru(2)–N(6) 2.152(7), Ru(2)–N(3) 2.167(7); N(2A)–Ru(1)–N(5) 85.1(2), N(4)–Ru(1)–N(5) 80.0(3), N(2A)–Ru(1)–N(4) 82.3(2), N(3)–Ru(2)–N(6) 79.4(3).

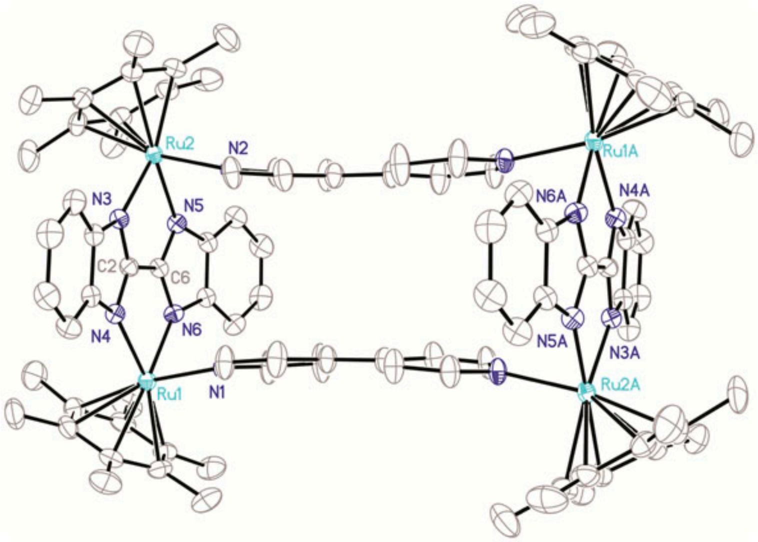

Figure 2. Molecular structure of **2** with thermal ellipsoids drawn at the 30% level. Hydrogens are omitted for clarity. Selected distances (Å) and angles (°): Ru(1)–N(1) 2.131(3), Ru(1)–N(4) 2.165(3), Ru(1)–N(6) 2.157(3), Ru(2)–N(2) 2.139(3), Ru(2)–N(3) 2.157(3), Ru(2)–N(5) 2.167(3); N(6)–Ru(1)–N(4) 79.23(12), N(1)–Ru(1)–N(6) 83.77(13), N(1)–Ru(1)–N(4) 84.29(12), N(3)–Ru(2)–N(5) 79.60(12).

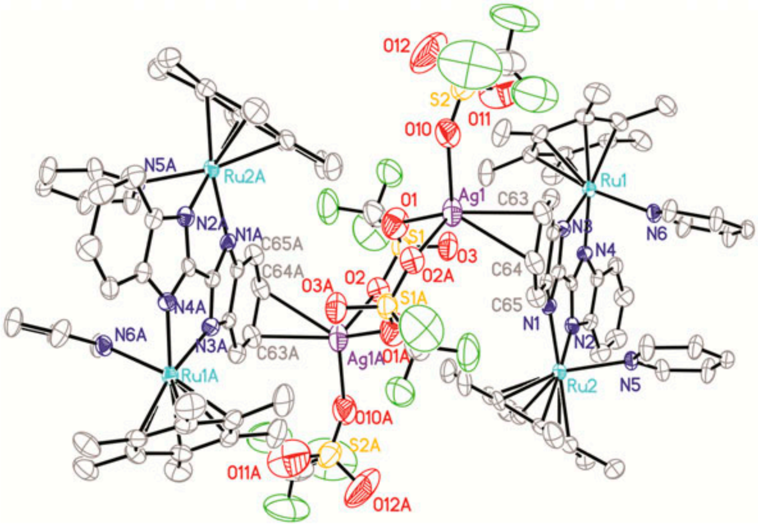

Figure 3. Molecular structure of **3** with thermal ellipsoids drawn at the 30% level. Hydrogens are omitted for clarity. Selected distances (Å) and angles (°): Ru(1)–N(3) 2.111(9), Ru(1)–N(4) 2.178(8), Ru(1)–N(6) 2.122(8), Ru(2)–N(1) 2.140(8), Ru(2)–N(2) 2.180(9), Ru(2)–N(5) 2.145(8), Ag(1)–O(1) 2.288(10), Ag(1)–O(10) 2.368(12), Ag(1)–O(2A) 2.477(10), Ag(1)–C(63) 2.487(12), Ag(1)–C(64) 2.700(12), S(1)–O(1) 1.390(11), S(1)–O(2) 1.411(10), S(1)–O(3) 1.448(11), C(63)–C(64) 1.401(16), C(64)–C(65) 1.361(16); N(3)–Ru(1)–N(4) 79.4(3), N(3)–Ru(1)–N(6) 85.1(3), N(6)–Ru(1)–N(4) 83.6(3), N(1)–Ru(2)–N(2) 79.3(3), O(1)–Ag(1)–O(10) 113.2(4), O(1)–Ag(1)–O(2A) 98.0(4), C(63)–Ag(1)–O(2A) 109.2(4), C(64)–Ag(1)–O(10) 113.6(4), C(63)–Ag(1)–C(64) 31.0(3), O(1)–S(1)–O(2) 116.5(7), O(1)–S(1)–O(3) 113.9(7), O(2)–S(1)–O(3) 115.2(7).

diagonal lengths (12.72 and 12.46 ppm) compared with those in [**1**][OTf]$_4$·4CH$_3$OH. The average Ru–N(BiBzIm) bond distance is 2.160(7) Å in [**1**][OTf]$_4$·4CH$_3$OH, similar to that in **2** (2.162(3) Å).

The molecular structure of **3** is shown in figure 3. The Ag–C bond distances are 2.487 (12) and 2.700(12) Å, respectively, comparable to those in related Ag–arene complexes (2.359(3)–2.764(6) Å) [23, 31]. The coordination geometry around silver(I) is pseudo-tetrahedral (taking the C=C group as one ligand), comprising three oxygens from three separate triflate ions (one terminal and two bridging) and one phenyl ring (η^2-carbon) of the BiBzIm. The μ_2,η^2-OTf coordination mode (type **c**) was first reported by Munakata in [Ag$_2$(HPB)(OTf)$_2$(toluene)] (HPB = hexaphenylbenzene) [32], in 1999. However, the [Ag$_2$(μ_2,η^2-OTf)$_2$(η^1-OTf)$_2$]$^{2-}$ bridging unit in **3** was observed only in the dimer [AgPPh$_2$(CH$_2$Py)(OTf)$_2$]$_2$ [33] and in the supramolecular capsule [(OTf)$_4$Ag$_8$(C≡C–C≡C)(Py6)$_2$]$^{2+}$ (Py6 = azacalix[6]pyridine) [34]. The Ag···Ag separation of 4.88 Å in **3** lies in the range of the above-mentioned silver complexes (4.64–5.78 Å) [33, 34]. The Ag–O bond lengths are between 2.288(10) and 2.477(10) Å, similar to those in related complexes (2.296–2.517 Å) [32–34]. The bond length of S(1)–O(3) (1.448(11) Å) is slightly longer than those of S(1)–O(1) (1.390(11) Å) and S(1)–O(2) (1.411(10) Å), indicating the S(1)–O$_{\text{terminal}}$ bond is more likely to be a single bond, contrary to those in [AgPPh$_2$(CH$_2$Py)(OTf)$_2$]$_2$ [33] and

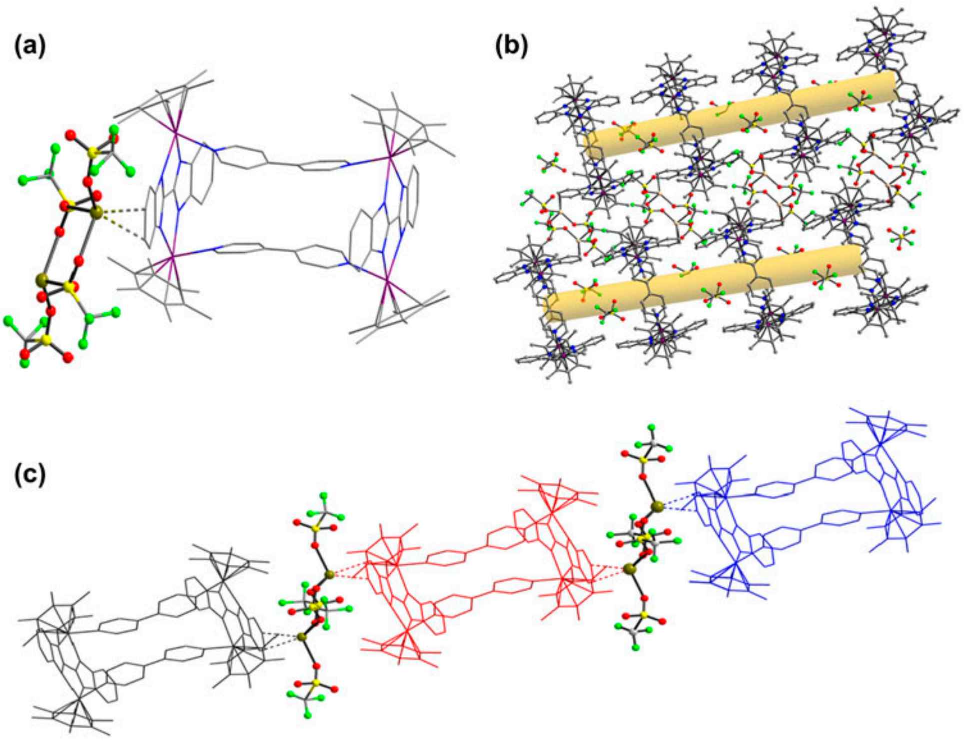

Figure 4. Hydrogens are omitted for clarity. (a) Interaction of **2** with [Ag$_2$(OTf)$_4$]$^{2-}$ in **3** (Ru: purple; Ag: yellowish brown; C: gray; O: red; N: blue; F: green; S: yellow); (b) Cell-packing network of **3** with ball and stick model; (c) Chain framework of **3**, the complex is a linear coordination polymer, where organometallic Ag–arene bonds link one molecule to the next (see http://dx.doi.org/10.1080/00958972.2014.966703 for color version).

$[(OTf)_4Ag_8(C{\equiv}C{-}C{\equiv}C)(Py6)_2]^{2+}$ [34]. The bond angle of O(1)–Ag(1)–O(2A) is 98.0(4)°, larger than those in $[Ag_2(HPB)(OTf)_2(toluene)]$ (97.0(3)°) [32] and $[AgPPh_2(CH_2Py)(OTf)_2]_2$ (91.58(5)°) [33]. The η^2-coordinating C=C bond distance in **3** (C(63)–C(64) 1.401 (16) Å) is slightly longer than that of corresponding free C=C bond in BiBzIm in **2** (1.379 or 1.386 Å). Figure 4(a) clearly illustrates the interaction between the tetranuclear metalla-rectangle **2** and the eight-membered $[Ag_2(OTf)_4]^{2-}$ core. From figure 4(b), **3** exists as a linear polymer with triflate anions either bonded to Ag(I) or non-bonded and sandwiched between the polymer chains. Figure 4(c) shows organometallic Ag–arene π bonds link one metalla-rectangle to the next. The dimensions of metalla-rectangles in **3** are 11.19 × 5.58 Å, similar to those in **2** (11.27 × 5.60 Å). The Ru(1)···Ru(1A) and Ru(2)···Ru(2A) diagonal length is 12.41 and 12.60 Å, respectively, slightly shorter than those in **2** (12.46 and 12.72 ppm).

The molecular structure of **4** is shown in figure 5, the dimensions of the metalla-rectangle are 13.21 × 3.73 Å, as defined by the ruthenium centers, and the Ru···Ru diagonal lengths are 13.98 and 13.46 Å, respectively. The dihedral angles of the two pyridyl groups out of the acenaphthylene plane are 89.5° and 81.0°, respectively. The silver center was chelated by four nitrogens from two *m*Py-bian ligands. The Ag(1)–N(1) and Ag(1)–N(2) bond lengths are 2.293(10) and 2.429(11) Å, respectively, shorter than the average Ag–N bond length in $[Cp^*{}_4Ir_4(BiBzIm)_2(m\text{Py-bian})_2Ag(H_2O)]^{5+}$ (2.462(11) Å) [28], indicating a more intense bonding of silver to nitrogen, possibly due to the shorter chloro-bridges in **4**. However, the average Ag–N bond distance of 2.361(10) Å in **4** lies in the range of related silver (I) α-diimine complexes $[Ag(o,o',p\text{-}Me_3C_6H_2\text{-bian})_2]BF_4$ (2.329(2) Å) and [Ag(*o*,*o*

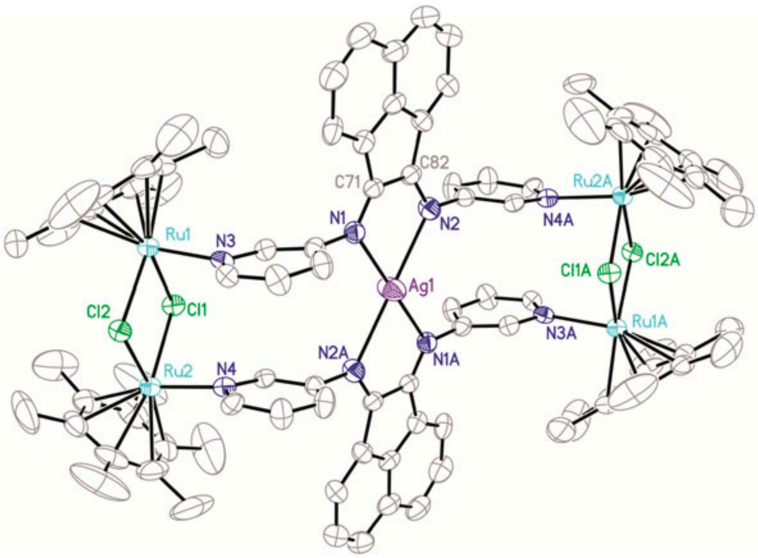

Figure 5. Molecular structure of **4** with thermal ellipsoids drawn at the 30% level. Hydrogens are omitted for clarity. Selected distances (Å) and angles (°): Ru(1)–N(3) 2.134(10), Ru(1)–Cl(1) 2.440(3), Ru(1)–Cl(2) 2.429(3), Ru(2)–N(4) 2.125(10), Ru(2)–Cl(1) 2.437(3), Ru(2)–Cl(2) 2.437(3), Ag(1)–N(1) 2.293(10), Ag(1)–N(2) 2.429(11), C(71)–N(1) 1.258(15), C(82)–N(2) 1.286(15); Cl(1)–Ru(1)–Cl(2) 80.19(10), N(3)–Ru(1)–Cl(1) 88.8(3), N(3)–Ru (1)–Cl(2) 86.8(3), Cl(2)–Ru(2)–Cl(1) 80.10(10), N(1)–Ag(1)–N(1A) 180.0(5), N(1)–Ag(1)–N(2) 71.6(4), N(2)–Ag (1)–N(2A) 180.000(2).

′-^{i}Pr$_2$C$_6$H$_3$-bian)$_2$]BF$_4$ (2.409(5) Å) [35]. The N(1)–Ag(1)–N(1A) and N(2)–Ag(1)–N(2A) bond angles are 180.0(5)$^\circ$ and 180.000(2)°, respectively, indicating a square-planar silver. Distorted tetrahedral environment is usually adopted for silver(I) α-diimine complexes, such as [Ag(*o*,*o*′,*p*-Me$_3$C$_6$H$_2$-bian)$_2$]BF$_4$ [35], Ag$_2$(H$_2$biim)$_4$(W$_6$O$_{19}$)·2H$_2$O (H$_2$biim = 2,2′-biimidazole) [36] and [Ag(**L2**)$_2$](BPh$_4$) (**L2** = 2,3,4,6,7,9,10,11-octahydro-pyrazino [1,2-a:4,3-a′] dipyrimidine) [37]. Complex **4** is the first case of Ag(I) diimine species with square-planar geometry. The N(1)–Ag(1)–N(2) bond angle is 71.6(4)°, larger than the corresponding N–Ag–N bond angles in [Cp*$_4$Ir$_4$(BiBzIm)$_2$(*m*Py-bian)$_2$Ag(H$_2$O)]$^{5+}$ (68.3(3), 70.2(4)°) [28], but near to those in [Ag(*o*,*o*′-^{i}Pr$_2$C$_6$H$_3$-bian)$_2$]BF$_4$ (2.409(5) Å) (71.7(2), 71.5(2)°) [35]. The average Ru–Cl bond length is 2.436(3) Å, comparable to those in other chloro-bridged metalla-rectangles [{Cp*$_2$Ir$_2$(μ-Cl)$_2$}$_2$(bpy)$_2$]$^{4+}$ and metallo-prisms [Ru$_6$(arene)$_6$(μ_3-tpt-κN)$_2$(μ-Cl)$_6$]$^{6+}$ (2.44–2.46 Å) [11, 29].

In summary, a new synthetic route was applied for construction of metalla-rectangles **1** and **2** in good yield. The 1-D mixed-metal network {[Ru$_4$(η^6-C$_6$Me$_6$)$_4$(bpy)$_2$(BiBzIm)$_2$·Ag$_2$(OTf)$_4$]$^{2+}$}$_n$ (**3**) comprises two fragments: tetranuclear rectangular structures **2** and [Ag$_2$(OTf)$_4$]$^{2-}$ units, which are linked by organometallic Ag–arene π bonds. The coordination geometry around silver(I) in **3** is pseudo-tetrahedral (taking the C=C group as one ligand), comprising three oxygens from three separate triflate ions (two bridging and one terminal) and one phenyl (η^2-carbon) from BiBzIm. The organometallic Ag–arene π bonds to connect metalla-rectangles might be another useful approach to design new heterometallic functionalized supramolecules. An unusal square-planar silver(I) is observed in the metalla-rectangle [(C$_6$Me$_6$)$_4$Ru$_4$(μ-Cl)$_4$(*m*Py-bian)$_2$Ag]$^{5+}$ (**4**) containing a silver(I) α-diimine moiety, and the isolation of chloro-bridged heterometallic metalla-rectangle indicated that silver(I) coordination occurred prior to the formation of the supposed intermediate [Cp*$_4$Ir$_4$(BiBzIm)$_2$(*m*Py-bian)$_2$]$^{4+}$ [28]. Self-assembly of arene-ruthenium building blocks with *m*Py-bian and other transition metal ions to prepare other heterometallic supramolecules are underway in the lab.

3. Experimental

3.1. *General considerations*

All operations were carried out under nitrogen using standard Schlenk techniques, and methanol and diethyl ether were distilled. Silver(I) trifluoromethanesulfonate and bpy were purchased from Energy Chemical Co., Inc. and used without purification. The starting materials *m*Py-bian [38], [(*p*-^{i}PrC$_6$H$_4$Me)RuCl$_2$]$_2$ [39], [(C$_6$Me$_6$)RuCl$_2$]$_2$ [40], and 2,2′-bisbenzimidazole [41] were prepared according to the literature. The ^{1}H NMR and ^{13}C NMR spectra were measured on a BrukerALX400 spectrometer in CD$_3$OD. Infrared spectra (KBr) were recorded on a Perkin Elmer 16 PC FT-IR spectrophotometer with pressed KBr pellets, and elemental analyses for C and H were carried out on an Elementar III Vario EI analyzer.

3.2. *Preparation of [Ru$_4$(arene)$_4$(bpy)$_2$(BiBzIm)$_2$]$^{4+}$ (arene = p-Pr^{i}C$_6$H$_4$Me 1, C$_6$Me$_6$ 2)*

2,2′-Bisbenzimidazole (11.7 mg, 0.05 mM) was added into a solution of [(*p*-^{i}PrC$_6$H$_4$Me) RuCl$_2$]$_2$ (31.2 mg, 0.05 mM)/[(C$_6$Me$_6$)RuCl$_2$]$_2$ (33.4 mg, 0.05 mM) in dry CH$_3$OH (8 mL) at room temperature. This was followed by stirring for 6 h, and then AgOTf (51.0 mg, 0.20 mM) was added to the solution to remove the chlorides from ruthenium for 6 h. The next step was mixing 4,4′-bipyridine (9.6 mg, 0.05 mM) with this suspension, and vigorous stirring was applied for 8 h. After the reaction was complete, the solution was filtered to remove undissolved materials. The pure product was obtained through the diffusion of ether into the filtrate after two days, giving crystals of **1** (orange, 46.0 mg, 80%) and **2** (red, 50.1 mg, 82%).

For **1**, IR(KBr): $\nu = 1632$(s, C=N), 1460(m), 1393(m), 1257(s), 1160 (m), 1117(s), 1030 (s), 641(s) cm^{-1}; ^{1}H NMR (400 Hz, methanol-d$_4$): $\delta = 0.90$ (d, $J = 6.8$ Hz, 24H, CH(CH_3)$_2$), 1.65 (s, 12H, ArCH$_3$), 2.46 (sept, 4H, CH(CH$_3$)$_2$), 6.17 (d, $J = 6.4$ Hz, 4H, p-^{i}PrC$_6$H$_4$Me), 6.62 (d, $J = 6.4$ Hz, 4H, p- ^{i}PrC$_6$H$_4$Me), 7.06 (d, $J = 6.4$ Hz, 8H, pyridyl), 7.59 (q, $J = 3.2$ Hz, 8H, BiBzIm), 7.81 (d, $J = 6.4$ Hz, 8H, pyridyl), 8.10 (q, $J = 3.2$ Hz, 8H, BiBzIm) ppm; ^{13}C NMR (100 Hz, methanol-d$_4$): $\delta = 18.04$ (CH(CH$_3$)$_2$), 22.57 (ArCH$_3$), 32.67 (CH(CH$_3$)$_2$), 79.80 (p-^{i}PrC$_6$H$_4$Me), 87.38 (p-^{i}PrC$_6$H$_4$Me), 103.86 (p-^{i}PrC$_6$H$_4$Me), 104.48 (p-^{i}PrC$_6$H$_4$Me), 117.33 (BiBzIm), 124.08 (bpy), 125.48 (BiBzIm), 145.71 (bpy), 145.74 (BiBzIm), 155.11 (C=N, bpy), 157.68 (N–C=N, BiBzIm) ppm; elemental Anal. Calcd (%) for $C_{92}H_{88}F_{12}N_{12}O_{12}Ru_4S_4$: C 47.75, H 3.83, N 7.26; found: C 47.80, H 3.86, N 7.30.

For **2**, IR(KBr): $\nu = 2115$(w), 1623(s, C = N), 1481(m), 1434(m), 1120 (m), 1091(s), 1030(s), 746(s), 696(m) cm^{-1}; ^{1}H NMR (400 Hz, methanol-d$_4$): $\delta = 2.26$ (s, 72H, CH$_3$), 6.97 (d, $J = 6.8$ Hz, 8H, pyridyl), 7.52 (q, $J = 3.2$ Hz, 8H, BiBzIm), 7.72 (d, $J = 6.8$ Hz, 8H, pyridyl), 7.94 (q, $J = 3.2$ Hz, 8H, BiBzIm) ppm; ^{13}C NMR (100 Hz, methanol-d$_4$): $\delta = 17.09$ (ArCH$_3$), 96.19 (C$_6$Me$_6$), 117.58 (BiBzIm), 123.79 (bpy), 124.95 (BiBzIm), 145.04 (bpy), 145.10 (BiBzIm), 154.30 (C = N, bpy), 157.85 (N–C=N, BiBzIm) ppm; elemental Anal. Calcd (%) for $C_{100}H_{104}F_{12}N_{12}O_{12}Ru_4S_4$: C 49.50, H 4.32, N 6.93; found: C 49.46, H 4.34, N 6.97.

3.3. *Preparation of* $\{[Ru_4(\eta^6\text{-}C_6Me_6)_4(bpy)_2(BiBzIm)_2{\cdot}Ag_2(OTf)_4]^{2+}\}_n$ *(3)*

Method A: 2,2′-Bisbenzimidazole (11.7 mg, 0.05 mM) was added to a solution of [(η^6-C$_6$Me$_6$)Ru(μ-Cl)Cl]$_2$ (33.4 mg, 0.05 mM) in dry CH$_3$OH (8 mL) at room temperature. This was followed by stirring for 6 h, and then AgOTf (76.0 mg, 0.30 mM) was added to the solution to remove the chlorides from ruthenium for 6 h. The next step was mixing 4,4′-bipyridine (9.6 mg, 0.05 mM) with this suspension, and vigorous stirring was applied for 8 h. After the reaction was complete, the suspension was filtered to remove undissolved materials. The pure product was obtained through diffusion of ether into the filtrate after one week, giving crystals of **3** (red, 7.3 mg, 20%). IR(KBr): $\nu = 2115$(w), 1623(s, C = N), 1479(m), 1434(m), 1120 (m), 1091(s), 1030(s), 743(s), 696(m) cm^{-1}; ^{1}H NMR (400 Hz, methanol-d$_4$): $\delta = 2.26$ (s, 72H, CH$_3$), 6.97 (d, $J = 6.8$ Hz, 8H, pyridyl), 7.63 (q, $J = 3.2$ Hz, 8H, BiBzIm), 7.72 (d, $J = 6.8$ Hz, 8H, pyridyl), 7.96 (q, $J = 3.2$ Hz, 8H, BiBzIm) ppm; elemental Anal. Calcd (%) for $C_{102}H_{104}Ag_2F_{18}N_{12}O_{18}Ru_4S_6$: C 41.67, H 3.57, N 5.72; found: C 41.70, H 3.58, N 5.77.

Method B: To a solution of **2** (48.0 mg, 0.02 mM) in methanol (10 mL) was added AgOTf (51.0 mg, 0.2 mM) with stirring for 12 h at room temperature. Then the suspension was filtered to remove undissolved materials. The pure product was obtained through diffusion of ether into the filtrate after two days, giving crystals of **3** (red, 8.8 mg, 15%). The determination of the unit cells is identified with the same complex obtained by Method A.

Table 1. Crystallographic data and experimental details for [**1**][OTf]$_4$·4CH$_3$OH, [**1**][OTf]$_4$, [**2**][OTf]$_4$, [**3**][OTf]$_{2n}$, and [**4**][OTf]$_5$.

	[**1**][OTf]$_4$·4CH$_3$OH	[**1**][OTf]$_4$	[**2**][OTf]$_4$	[**3**][OTf]$_{2n}$	[**4**][OTf]$_5$
Formula	$C_{96}H_{104}F_{12}N_{12}O_{16}Ru_4S_4$	$C_{92}H_{88}F_{12}N_{12}O_{12}Ru_4S_4$	$C_{100}H_{104}F_{12}N_{12}O_{12}Ru_4S_4$	$C_{102}H_{104}Ag_2F_{18}N_{12}O_{18}Ru_4S_6$	$C_{97}H_{100}AgCl_4F_{15}N_8O_{15}Ru_4S_5$
Fw	2442.43	2314.26	2426.47	2940.35	2717.10
T (K)	296(2)	296(2)	296(2)	296(2)	296(2)
Cryst. syst.	Monoclinic	Monoclinic	Monoclinic	Triclinic	Triclinic
Space group	*P2₁/c*	*P2₁/c*	*C2/c*	*P-1*	*P-1*
a (Å)	18.65(3)	18.536(6)	22.636(3)	12.3964(19)	11.215(8)
b (Å)	19.05(3)	18.906(11)	15.4134(18)	16.117(3)	12.035(8)
c (Å)	18.00(3)	18.153(12)	32.927(4)	17.755(3)	21.285(14)
α (°)	90	90	90	101.603(2)	101.260(8)
β (°)	115.895(19)	106.039(8)	95.638(2)	93.951(2)	98.132(9)
γ (°)	90	90	90	110.097(2)	98.307(9)
Volume (Å^3)	5753(15)	5716(6)	11,432(2)	3226.4(9)	2745(3)
Z	2	2	4	1	1
D_{Calcd}, Mg m^{-3}	1.410	1.345	1.410	1.513	1.643
Absorp. coeff. (mm^{-1})	0.668	0.666	0.670	0.938	0.994
F (0 0 0)	2480	2336	4928	1472	1364
2θ range (°)	2.43–27.48	2.25–27.56	2.389–27.552	2.27–25.00	2.26–25.00
No. of reflns. collected/unique	32,130/12,593 [R(int) = 0.1142]	34,651/13,118 [R(int) = 0.1113]	35,016/13,042 [R(int) = 0.0410]	16,117/10,933 [R(int) = 0.0514]	13,531/9430 [R(int) = 0.0728]
No. of data/restraints/ parameters	12,593/700/659	13,118/697/619	13,042/26/625	10,933/796/742	9430/842/685
Goodness-of-fit on F^2	0.917	0.851	1.091	1.028	0.928
Final *R* indices [$I > 2\sigma(I)$]^a	$R_1 = 0.0809$ $wR_2 = 0.2062$	$R_1 = 0.0804$ $wR_2 = 0.1931$	$R_1 = 0.0539$ $wR_2 = 0.1561$	$R_1 = 0.0855$ $wR_2 = 0.2017$	$R_1 = 0.1035$ $wR_2 = 0.2767$
Largest diff. peak/hole, e Å^{-3}	0.922/–0.972	0.642/–0.364	2.111/–1.182	0.983/–0.921	1.774/–1.816

$^a R_1 = \|F_o| - |F_c\|/\sum|F_o|$; $wR_2 = [\sum w(|F_o^2| - |F_c^2|)^2/\sum w|F_o^2|^2]^{1/2}$.

3.4. *Preparation of $[(\eta^6\text{-}C_6Me_6)Ru_4(\mu\text{-}Cl)_4(mPy\text{-}bian)_2Ag]^{5+}$ (4)*

AgOTf (38.2 mg, 0.15 mM) was added into the solution of $[(\eta^6\text{-}C_6Me_6)Ru(\mu\text{-}Cl)Cl]_2$ (33.4 mg, 0.05 mM) in dry CH_3OH (8 mL) at room temperature for 4 h. The next step was mixing *m*Py-bian (16.7 mg, 0.05 mM) with this suspension, and vigorous stirring was applied for 8 h. After the reaction was complete, the solution was filtered to remove undissolved materials. The pure product was obtained through the diffusion of ether into the filtrate after one week, giving crystals of **4** (orange, 20.0 mg, 30%). IR(KBr): $\nu = 1608$ (m, C=N), 1457(m), 1391(w), 1256(s), 1160 (m), 1031(m), 751(m), 640(m) cm^{-1}; ^1H NMR (400 Hz, methanol-d_4): $\delta = 2.24$ (s, 72H, CH_3), 6.70 (d, $J = 7.2$ Hz, 2H), 7.01 (d, $J = 7.2$ Hz, 2H), 7.57–7.62 (m, 4H), 7.67–7.79 (m, 8H), 7.93–7.96 (m, 2H), 8.20–8.27 (m, 8H), 8.98–9.08 (m, 2H); elemental Anal. Calcd (%) for $C_{97}H_{100}AgCl_4F_{15}N_8O_{15}Ru_4S_5$: C 42.88, H 3.71, N 4.12; found: C 42.83, H 3.73, N 4.15.

3.5. *X-ray diffraction measurements*

Single crystals of **1**·$4CH_4O$ and **1–3** suitable for X-ray analysis were sealed into a glass capillary in case they effloresced. Crystals of **4** were stable in air. Intensity data were collected on a Bruker SMART APEX 2000 CCD diffractometer using graphite-monochromated Mo Kα radiation ($\lambda = 0.71073$ Å). The collected frames were processed with the software SAINT [42]. The data were corrected for absorption using SADABS [43]. Structures were solved by direct methods and refined by full-matrix least-squares on F^2 using the SHELXTL software package [44, 45]. All non-hydrogen atoms were refined anisotropically. The positions of all hydrogens were generated geometrically (C_{sp3}-H = 0.96, C_{sp2}-H = 0.93), assigned isotropic thermal parameters, and allowed to ride on their respective parent carbon or oxygen before the final cycle of least-squares refinement. In **1–4**, there are disordered solvents and/or anions in the voids of the crystal structure. Hence, new data-sets corresponding to omission of the disordered anions and solvents were generated with the SQUEEZE [46] algorithm, and the structures were refined to convergence. Crystallographic data and experimental details for **1**·$4CH_4O$, **1**, **2**, **3**, and **4** are given in table 1.

Supplementary material

CCDC 1005561, 996686, 996750, 996751 and 996759 contain the supplementary crystallographic data for **1**·$4CH_4O$, **1**, **2**, **3,** and **4** and can be obtained free of charge from the Cambridge Crystallographic Data Center via www.ccdc.cam.ac.uk/data_request/cif.

Funding

This project was supported by the Natural Science Foundation of China [grant number 21201003] and [grant number 21372007].

References

[1] T.R. Cook, Y.R. Zheng, P.J. Stang. *Chem. Rev.*, **113**, 734 (2013).
[2] A. Mishra, S. Lee, H. Kim, T.R. Cook, P.J. Stang, K.W. Chi. *Chem.-Asian J.*, **7**, 2592 (2012).
[3] M.C. Dul, E. Pardo, R. Lescouëzec, Y. Journaux, J. Ferrando-Soria, R. Ruiz-García, J. Cano, M. Julve, F. Lloret, D. Cangussu, C.L.M. Pereira, H.O. Stumpf, J. Pasán, C. Ruiz-Pérez. *Coord. Chem. Rev.*, **254**, 2281 (2010).

[4] Y.F. Han, W.G. Jia, Y.J. Lin, G.-X. Jin. *Angew. Chem., Int. Ed.*, **48**, 6234 (2009).

[5] M.A. Furrer, A. Garci, E. Denoyelle-Di-Muro, P. Trouillas, F. Giannini, J. Furrer, C.M. Clavel, P.J. Dyson, G. Süss-Fink, B. Therrien. *Chem.-Eur. J.*, **19**, 3198 (2013).

[6] C.J. Hastings, M.P. Backlund, R.G. Bergman, K.N. Raymond. *Angew. Chem., Int. Ed.*, **50**, 10570 (2011).

[7] S.-L. Huang, Y.-J. Lin, T.S.A. Hor, G.-X. Jin. *J. Am. Chem. Soc.*, **135**, 8125 (2013).

[8] B. Kilbas, S. Mirtschin, R. Scopelliti, K. Severin. *Chem. Sci.*, **3**, 701 (2012).

[9] R. Chakrabarty, P.S. Mukherjee, P.J. Stang. *Chem. Rev.*, **111**, 6810 (2011).

[10] J. Mattsson, P. Govindaswamy, A.K. Renfrew, P.J. Dyson, P. Štěpnička, G. Süss-Fink, B. Therrien. *Organometallics*, **28**, 4350 (2009).

[11] P. Govindaswamy, G. Süss-Fink, B. Therrien. *Organometallics*, **26**, 915 (2007).

[12] A. Granzhan, C. Schouwey, T. Riis-Johannessen, R. Scopelliti, K. Severin. *J. Am. Chem. Soc.*, **133**, 7106 (2011).

[13] V. Vajpayee, S. Lee, J.W. Park, A. Dubey, H. Kim, T.R. Cook, P.J. Stang, K.-W. Chi. *Organometallics*, **32**, 1563 (2013).

[14] S. Shanmugaraju, A.K. Bar, P.S. Mukherjee. *Inorg. Chem.*, **49**, 10235 (2010).

[15] Y.-F. Han, Y.-J. Lin, L.-H. Weng, H. Berke, G.-X. Jin. *Chem. Commun.*, 350 (2008).

[16] G.A. Timco, E.J.L. McInnes, R.E.P. Winpenny. *Chem. Soc. Rev.*, **42**, 1796 (2013).

[17] Y.-Y. Zhang, Y.-J. Lin, G.-X. Jin. *Chem. Commun.*, **50**, 2327 (2014).

[18] M.N. Kozlova, S. Ferlay, S.E. Solovieva, I.S. Antipin, A.I. Konovalov, N. Kyritsakas, M.W. Hosseini. *Dalton Trans.*, 5126 (2007).

[19] G.L. Wang, Y.J. Lin, G.X. Jin. *Dalton Trans.*, **40**, 5166 (2011).

[20] B. Li, S.-Q. Zang, H.-Y. Li, Y.-J. Wu, T.C.W. Mak. *J. Organomet. Chem.*, **708**, 112 (2012).

[21] F.-B. Xu, Q.-S. Li, L.-Z. Wu, X.-B. Leng, Z.-C. Li, X.-S. Zeng, Y.L. Chow, Z.-Z. Zhang. *Organometallics*, **22**, 633 (2003).

[22] P. Pérez-Galán, N. Delpont, E. Herrero-Gómez, F. Maseras, A.M. Echavarren. *Chem.-Eur. J.*, **16**, 5324 (2010) and references therein.

[23] M. Munakata, L.P. Wu, T. Kuroda-Sowa, M. Maekawa, Y. Suenaga, K. Sugimoto. *Inorg. Chem.*, **36**, 4903 (1997).

[24] D.D.J.W. Mercer, H.A. Jenkins. *Inorg. Chim. Acta*, **360**, 3091 (2007).

[25] Y. Oka, N. Tamaoki. *Inorg. Chem.*, **49**, 4765 (2010).

[26] I. Ino, L.P. Wu, M. Munakata, T. Kuroda-Sowa, M. Maekawa, Y. Suenaga, R. Sakai. *Inorg. Chem.*, **39**, 5430 (2000).

[27] A. Gogoll, P. Polavarapu, H. Grennberg. *Inorg. Chem.*, **46**, 5271 (2007).

[28] T. Wu, Y.J. Lin, G.X. Jin. *Dalton Trans.*, **42**, 82 (2013).

[29] J.-Q. Wang, C.-X. Ren, G.-X. Jin. *Organometallics*, **25**, 74 (2006).

[30] P.H. Dinolfo, M.E. Williams, C.L. Stern, J.T. Hupp. *J. Am. Chem. Soc.*, **126**, 12989 (2004).

[31] J.-H. Son, M.A. Pudenz, J.D. Hoefelmeyer. *Dalton Trans.*, **39**, 11081 (2010).

[32] G.L. Ning, M. Munakata, L.P. Wu, M. Maekawa, Y. Suenaga, T. Kuroda-Sowa, K. Sugimoto. *Inorg. Chem.*, **38**, 5668 (1999).

[33] R.P. Feazell, C.E. Carson, K.K. Klausmeyer. *Inorg. Chem. Commun.*, **9**, 418 (2006).

[34] C.-Y. Gao, L. Zhao, M.-X. Wang. *J. Am. Chem. Soc.*, **134**, 824 (2012).

[35] V. Rosa, C.I.M. Santos, R. Welter, G. Aullón, C. Lodeiro, T. Avilés. *Inorg. Chem.*, **49**, 8699 (2010).

[36] P. Zhang, J. Peng, H. Pang, J. Sha, M. Zhu, D. Wang, M. Liu. *CrystEngComm*, **13**, 3832 (2011).

[37] J. Li, D.W. Widlicka, K. Fichter, D.P. Reed, G.R. Weisman, E.H. Wong, A. DiPasquale, K.J. Heroux, J.A. Golen, A.L. Rheingold. *Inorg. Chim. Acta*, **364**, 185 (2010).

[38] J. Flapper, J.N.H. Reek. *Angew. Chem. Int. Ed.*, **46**, 8590 (2007).

[39] M.A. Bennett, A.K. Smith. *J. Chem. Soc., Dalton Trans.*, 233 (1974).

[40] M.A. Bennett, T.-N. Huang, T.W. Matheson, A.K. Smith. *Inorganic Syntheses*, Vol. 21, p. 74.Wiley, New York (1982).

[41] H.J. Tang, G.Z. Zhang, C.J. Cong, K.L. Zhang. *Huaxue Shiji*, **29**, 733 (2007).

[42] G.M. Sheldrick. *SADABS*, University of Göttingen (1996).

[43] *SMART and SAINT+ for Windows NT (Version 6.02a)*, Bruker Analytical X-ray Instruments Inc., Madison, WI (1998).

[44] G.M. Sheldrick. *SHELXTL Software Reference Manual (Version 5.1)*, Bruker AXS Inc., Madison, WI (1997).

[45] G.M. Sheldrick. *Acta Crystallogr., Sect. A*, **64**, 112 (2008).

[46] *PLATON Program: A Multi-Purpose Crystallographic Tool*, Utrecht University, Utrecht. See: A.L. Spek. *Acta Crystallogr., Sect. A*, **46**, C34 (1990).